FTUV/98-35; IFIC/98-36

Nuclear effects in the F_3 structure function

E. Marco, E. Oset and S.K. Singh*
Departamento de Física Teórica and IFIC,
Centro Mixto Universidad de Valencia-CSIC,
46100 Burjassot (Valencia), Spain
(February 9, 2008)

Abstract

By using a relativistic framework and accurate nuclear spectral functions we evaluate the ratio F_{3A}/AF_{3N} of deep inelastic neutrino scattering. Parametrizations of this ratio for different values of Q^2 are provided. These results should be useful for taking into account the nuclear effects in analyses of experimental data in neutrino reactions in nuclear targets, and test QCD predictions for the nucleon structure functions. In particular, the size of the nuclear corrections is of the same order of magnitude as the size of the QCD corrections to the Gross-Llewellyn Smith sum rule.

13.15.+g, 24.10.-i, 24.85.+p, 25.30.-c, 25.30.Pt

Typeset using REVTEX

I. INTRODUCTION

The deep inelastic scattering (DIS) experiments done with neutrino beams can now provide data with an accuracy comparable to the analogous processes studied with charged leptons [1,2]. Due to the low cross sections, for neutrino interaction with matter, these data are collected mostly from experiments done on heavy nuclei like iron [2].

Since the discovery of the EMC effect [3], the deviation of the nuclear structure function $F_2^l(x)$ with respect to the deuteron, many theoretical attempts were made to explain it (for a review see [4–6]). In the conventional nuclear physics models, the usual effects considered are Fermi motion [7] and binding of the nucleons in the nuclei [8] and the contribution of the virtual meson cloud [9,10].

For the neutrino processes, the study of possible nuclear effects has received much less attention, probably because of the lack of accurate measurements in the past. In present analyses of neutrino experiments, the high x data ($x > 0.7$), where Fermi motion effects are expected to be important [7], are generally avoided, especially in the case of nuclear data [2]. However, it has been shown that even in the case of the deuteron, the Fermi motion effects could be important [11]. It is interesting to note that the older fits of Diemoz et al. [12], show that even for lower x ($x \approx 0.5$), the nuclear effects could be important. Most of the analyses done for the neutrino data assume the same nuclear corrections as applicable to the charged lepton experiments in their global fits of the parton distributions [13,14], while allowing for an overall normalisation of the data. This is not appropriate for the parity violating structure function $F_{3A}^\nu(x)$, in the neutrino scattering data, which has no counterpart in the charged lepton case. Even in the case of the structure function $F_{2A}^\nu(x)$, which is related to the $F_{2A}^l(x)$, of the EMC effect, the nuclear corrections would not be the same due to the different contribution of the sea quarks [15].

Recently, there have been some calculations of the nuclear effects in the $F_{3A}^\nu(x)$ structure function [16,17]. It is found by Sidorov and Tokarev (ST) [16] that the nuclear effects in $F_3^\nu(x)$ are quite small in the case of the deuteron, a result similar to the one found in charged lepton scattering in $F_{2D}^l(x)$ [18,19]. Keeping in view the result that the nuclear effects in $F_2^l(x)$ are quite different for the deuteron and heavy nuclei, the assumption that they are the same for $F_3^\nu(x)$, as done by ST is therefore not justified.

In the calculation of Kulagin [17], the iron structure function is evaluated and sizeable deviations from the deuteron one were found. The effect on the Gross-Llewellyn Smith (GLS) sum rule [20] is on the contrary very small. This is so because in Kulagin's approach, the spinors are normalized in order not to affect this sum rule. It is similar to the prescription introduced by means of the so called flux factor [21] in order to take into account relativistic effects in non relativistic formalisms. It is interesting to note that in the fit that the CCFR collaboration made to the $xF_2(x)$ and $xF_3(x)$ neutrino data [2,22], the integral of the valence quark distributions is not 3, [22]. This apparent lack of normalization of the $F_{3A}(x)$ in the nuclear data is of crucial importance in order to extract the strong coupling constant, α_s, from the analysis of the GLS sum rule, as done in [23].

Recently, a new calculation of the nuclear effects in the case of the charged lepton scattering was made [10,24]. In this calculation a relativistic many-body approach for the nucleon contribution was developed in order to avoid the use of the flux factor mentioned before [21]. The meson cloud contribution was found to give relatively important contributions. Good

agreement was found with the experimental data. For the structure function $F_{3A}(x)$, the virtual meson cloud gives no contribution, since it is related to the difference of the quark and antiquark distributions. In the present paper we calculate the nuclear effects to $F_{3A}(x)$ in the same formalism of [10,24].

The structure of the paper is as follows. We briefly present the formalism for deep inelastic neutrino scattering in section II. In section III we show how nuclear effects are calculated. In section IV we present the results and state our conclusions.

II. DEEP INELASTIC NEUTRINO-NUCLEON SCATTERING

The invariant matrix element for the Feynman diagram shown in Fig. 1 corresponding to the inelastic neutrino-nucleon scattering is written as

$$-\,iT = \left(\frac{iG}{\sqrt{2}}\right) \bar{u}_\mu(\boldsymbol{k}')\gamma^\alpha(1-\gamma_5)u_\nu(\boldsymbol{k}) \left(\frac{m_W^2}{q^2-m_W^2}\right) \langle X|J_\alpha|N\rangle \,. \tag{1}$$

The cross section for the neutrino scattering, σ^ν, is then given by

$$\begin{aligned}\sigma^\nu = {} & \frac{1}{v_{rel}}\frac{2m_\nu}{2E_\nu(\boldsymbol{k})}\frac{2M}{2E(\boldsymbol{p})}\int\frac{d^3k'}{(2\pi)^3}\frac{2m_\mu}{2E_\mu(\boldsymbol{k}')} \\ & \times\prod_{i=1}^{N}\int\frac{d^3p_i'}{(2\pi)^3}\prod_{l\epsilon f}\left(\frac{2M_l'}{2E_l'}\right)\prod_{j\epsilon b}\left(\frac{1}{2\omega_j'}\right)\bar{\sum}\sum|T|^2 \\ & \times(2\pi)^4\delta^4(p+k-k'-\sum_{i=1}^{N}p_i')\,,\end{aligned} \tag{2}$$

where f stands for fermions and b for bosons in the final state X. The index i is split in l, j for fermions and bosons respectively.

By inserting expression (1) in Eq. (2), summing over the final spins and averaging over the initial spins, the cross section can be expressed in the rest frame of the nucleon, with Ω', E' referring to the outgoing muon, as

$$\frac{d^2\sigma^\nu}{d\Omega' dE'} = \frac{G^2}{(2\pi)^2}\frac{|\boldsymbol{k}'|}{|\boldsymbol{k}|}\left(\frac{m_W^2}{q^2-m_W^2}\right)^2 [L^{\alpha\beta}+L_5^{\alpha\beta}]\, W^\nu_{\alpha\beta}\,, \tag{3}$$

where the lepton tensors, $L^{\alpha\beta}$ and $L_5^{\alpha\beta}$ are given by

$$\begin{aligned} L^{\alpha\beta} &= k^\alpha k'^\beta + k^\beta k'^\alpha - (kk')g^{\alpha\beta}\,, \\ L_5^{\alpha\beta} &= -i\epsilon^{\alpha\beta\rho\sigma}k_\rho k'_\sigma\,, \end{aligned} \tag{4}$$

and the hadronic tensor is defined as

$$\begin{aligned} W^\nu_{\alpha\beta} = {} & \frac{1}{2\pi}\bar{\sum_{s_p}}\sum_X\sum_{s_i}\prod_{i=1}^{N}\int\frac{d^3p_i'}{(2\pi)^3}\prod_{l\epsilon f}\left(\frac{2M_l'}{2E_l'}\right)\prod_{j\epsilon b}\left(\frac{1}{2\omega_j'}\right) \\ & \times\langle X|J_\alpha|N\rangle\langle X|J_\beta|N\rangle^*(2\pi)^4\delta^4(p+q-\sum_{i=1}^{N}p_i')\,, \end{aligned} \tag{5}$$

where q is the momentum of the virtual W, s_p the spin of the nucleon and s_i the spin of the fermions in X.

In the case of antineutrino scattering, the invariant T matrix is given by

$$-\,iT = \left(\frac{iG}{\sqrt{2}}\right) \bar{v}_\nu(\boldsymbol{k})\gamma^\alpha(1-\gamma_5)v_\mu(\boldsymbol{k'}) \left(\frac{m_W^2}{q^2-m_W^2}\right) \langle X|J_\alpha^\dagger|N\rangle \tag{6}$$

and the cross section reads

$$\frac{d^2\sigma^{\bar{\nu}}}{d\Omega' dE'} = \frac{G^2}{(2\pi)^2}\,\frac{|\boldsymbol{k'}|}{|\boldsymbol{k}|}\,\left(\frac{m_W^2}{q^2-m_W^2}\right)^2 [L^{\alpha\beta} - L_5^{\alpha\beta}]\, W^{\bar{\nu}}_{\alpha\beta}\,. \tag{7}$$

The usual convention is to express the hadronic tensor as [25]

$$\begin{aligned} W^{\nu(\bar{\nu})}_{\alpha\beta} = & \left(\frac{q_\alpha q_\beta}{q^2} - g_{\alpha\beta}\right)\, W_1^{\nu(\bar{\nu})} + \frac{1}{M^2}\left(p_\alpha - \frac{pq}{q^2}\,q_\alpha\right)\left(p_\beta - \frac{p.q}{q^2}\,q_\beta\right) W_2^{\nu(\bar{\nu})} \\ & - \frac{i}{2M^2}\epsilon_{\alpha\beta\rho\sigma}p^\rho q^\sigma W_3^{\nu(\bar{\nu})} + \frac{1}{M^2}q_\alpha q_\beta W_4^{\nu(\bar{\nu})} \\ & + \frac{1}{M^2}(p_\alpha q_\beta + q_\alpha p_\beta)W_5^{\nu(\bar{\nu})} + \frac{i}{M^2}(p_\alpha q_\beta - q_\alpha p_\beta)W_6^{\nu(\bar{\nu})}\,, \end{aligned} \tag{8}$$

where $W_i^{\nu(\bar{\nu})}$ are the structure functions, which depend on the scalars q^2 and pq. The terms depending on W_4, W_5 and W_6 in Eq. (8) do not contribute to the cross section in the DIS [25].

Defining the variables

$$Q^2 = -q^2; \quad \nu = \frac{pq}{M}; \quad x = \frac{Q^2}{2M\nu}; \quad y = \frac{\nu}{E_\nu(\boldsymbol{k})}\,, \tag{9}$$

we can write in the Bjorken limit

$$\frac{d^2\sigma^{\nu(\bar{\nu})}}{dxdy} = \frac{G^2 M E_\nu(\boldsymbol{k})}{\pi}\left\{xy^2F_1^{\nu(\bar{\nu})}(x) + \left(1 - y - \frac{xyM}{2E_\nu(\boldsymbol{k})}\right)F_2^{\nu(\bar{\nu})}(x) \pm xy(1-y/2)F_3^{\nu(\bar{\nu})}(x)\right\}\,, \tag{10}$$

where the + (−) sign stands for the neutrino (antineutrino) cross section, and the $F_i^{\nu(\bar{\nu})}(x)$ are dimensionless structure functions defined as

$$F_1^{\nu(\bar{\nu})} = MW_1^{\nu(\bar{\nu})}; \quad F_2^{\nu(\bar{\nu})} = \nu W_2^{\nu(\bar{\nu})}; \quad F_3^{\nu(\bar{\nu})} = \nu W_3^{\nu(\bar{\nu})}\,. \tag{11}$$

In the quark parton model, the structure functions are expressed in terms of the quark distributions, $q(x)$ and $\bar{q}(x)$. Using Callan-Gross relation, these structure functions are given as

$$2xF_{1N}^\nu = 2xF_{1N}^{\bar{\nu}} = F_{2N}^\nu = F_{2N}^{\bar{\nu}} = x(q(x) + \bar{q}(x))\,,$$

$$F_{3N}^\nu = q(x) - \bar{q}(x) + 2s(x) - 2c(x)\,,$$

$$F_{3N}^{\bar{\nu}} = q(x) - \bar{q}(x) - 2s(x) + 2c(x)\,,$$

$$F_3(x) = \frac{1}{2}[F_{3N}^{\nu}(x) + F_{3N}^{\bar{\nu}}(x)] = q(x) - \bar{q}(x) = u_v(x) + d_v(x)\,. \quad (12)$$

Here

$$\begin{aligned} q(x) &= u(x) + d(x) + s(x) + c(x) \\ \bar{q}(x) &= \bar{u}(x) + \bar{d}(x) + \bar{s}(x) + \bar{c}(x)\,. \end{aligned} \quad (13)$$

The neutrino structure function F_{2N}^{ν} is related with the analogous one for charged lepton scattering F_{2N}^{l} by

$$\frac{F_{2N}^{l}}{F_{2N}^{\nu}} = \frac{5}{18}\left(1 - \frac{3}{5}\frac{s(x) + \bar{s}(x) - c(x) - \bar{c}(x)}{q(x) + \bar{q}(x)}\right)\,. \quad (14)$$

In the deep inelastic region, quark distributions satisfy sum rules in order to give the correct charge, strangeness and charm of the proton and the neutron. This implies the constraint

$$\int_0^1 F_3(x)\,dx = 3\,, \quad (15)$$

known as the Gross-Llewellyn Smith (GSL) sum rule [20].

QCD corrections modify the expression of the structure functions in terms of the quark distributions, Eqs. (12). At leading order, Eqs. (12) retain the same structure but the quark distributions evolve with Q^2 according to the DGLAP (Dokshitzer-Gribov-Lipatov-Altarelli-Parisi) evolution equations [26]. When higher orders are considered, Eqs. (12) are modified including explicitly the strong coupling constant, $\alpha_S(Q^2)$.

The GLS sum rule is modified and in the NLO approximation is given by

$$\int_0^1 F_3(x)\,dx = 3(1 - \frac{\alpha_S(Q^2)}{\pi})\,. \quad (16)$$

Further higher order corrections up to order $\alpha_S^3(Q^2)$ can be found in [27].

III. NUCLEAR EFFECTS IN NEUTRINO SCATTERING

In order to calculate the neutrino-nucleus cross section we first evaluate the related neutrino self-energy in the medium, Fig. 2. The self-energy is given by

$$\begin{aligned} -i\Sigma(k) = &-\frac{G}{\sqrt{2}}\int\frac{d^4q}{(2\pi)^4}\,\bar{u}_\nu(\boldsymbol{k})\gamma_\beta(1-\gamma_5)\,i\frac{\not{k}' + m_\mu}{k'^2 - m_\mu^2 + i\epsilon}\,\gamma_\alpha(1-\gamma_5)u_\nu(\boldsymbol{k}) \\ &\times\left(\frac{-im_W}{q^2 - m_W^2}\right)^2\,(-i)\,\Pi^{\alpha\beta}(q)\,, \end{aligned} \quad (17)$$

where $\Pi^{\alpha\beta}(q)$ is the W self-energy in the medium.

Eq. (17) can be rewritten in the form

$$\Sigma(k) = \frac{iG}{\sqrt{2}} \frac{4}{m_\nu} \int \frac{d^4q}{(2\pi)^4} \frac{L^{\alpha\beta} + L_5^{\alpha\beta}}{k'^2 - m_\mu^2 + i\epsilon} \left(\frac{m_W}{q^2 - m_W^2} \right)^2 \Pi_{\alpha\beta}(q) \,. \tag{18}$$

The probability per unit time for the neutrino to collide with nucleons when travelling through nuclear matter is [10]

$$\Gamma(k) = -\frac{2m_\nu}{E_\nu(\boldsymbol{k})} \,\mathrm{Im}\, \Sigma(k) \,, \tag{19}$$

and the cross section for an element of volume d^3r in the nucleus is

$$\begin{aligned} d\sigma &= \Gamma dt dS = \Gamma \frac{dt}{dl} \, dl dS = \frac{\Gamma}{v} \, d^3r = \\ &= \Gamma \, \frac{E_\nu(\boldsymbol{k})}{|\boldsymbol{k}|} \, d^3r = -\frac{2m_\nu}{|\boldsymbol{k}|} \,\mathrm{Im}\, \Sigma \; d^3r \,. \end{aligned} \tag{20}$$

Im Σ can be easily evaluated from Eq. (18) by means of the Cutkosky rules [28]

$$\begin{array}{lcl} \Sigma(k) & \rightarrow & 2i \,\mathrm{Im}\, \Sigma(k) \\ D(k') & \rightarrow & 2i\theta(k'^0) \,\mathrm{Im}\, D(k') \text{ (boson propagator)} \\ \Pi^{\mu\nu}(q) & \rightarrow & 2i\theta(q^0) \,\mathrm{Im}\, \Pi^{\mu\nu}(q) \\ G(p) & \rightarrow & 2i\theta(p^0) \,\mathrm{Im}\, G(p) \text{ (fermion propagator)} \end{array} \tag{21}$$

and we get

$$\frac{d^2\sigma^\nu}{d\Omega' dE'} = -\frac{G}{\sqrt{2}} \frac{4}{(2\pi)^3} \frac{|\boldsymbol{k}'|}{|\boldsymbol{k}|} \left(\frac{m_W}{q^2 - m_W^2} \right)^2 [L^{\alpha\beta} + L_5^{\alpha\beta}] \int d^3r \,\mathrm{Im}\, \Pi_{\alpha\beta}(q) \,. \tag{22}$$

Comparing Eq. (3) and Eq. (22) we see that

$$W_A^{\alpha\beta}(q) = -\frac{\sqrt{2}}{\pi} \frac{1}{G m_W^2} \int d^3r \,\mathrm{Im}\, \Pi^{\alpha\beta}(q) \,. \tag{23}$$

Next, we evaluate the W self-energy in the medium

$$\begin{aligned} -i\Pi^{\alpha\beta}(q) = (-) \int \frac{d^4p}{(2\pi)^4} \, iG(p) \sum_X \sum_{s_p, s_i} \prod_{i=1}^N \int \frac{d^4p'_i}{(2\pi)^4} \\ \times \prod_l iG_l(p'_l) \prod_j iD_j(p'_j) \left(\frac{-G m_W^2}{\sqrt{2}} \right) \langle X|J^\alpha|N\rangle \langle X|J^\beta|N\rangle^* \\ \times (2\pi)^4 \delta^4(q + p - \Sigma_{i=1}^N p'_i) \,, \end{aligned} \tag{24}$$

where we have a minus sign because of the necessary fermion loop. In the antineutrino case the expressions obtained are very similar. $L_5^{\alpha\beta}$ appears, as in Eq. (7), with a minus sign in front and in the W self-energy, Eq. (24), we have $\langle X|J_\alpha^\dagger|N\rangle$, instead of $\langle X|J_\alpha|N\rangle$. From now on we will always speak of the average of neutrino and antineutrino structure functions and will omit the superscripts ν and $\bar{\nu}$. For the nucleon propagator in the medium, $G(p)$, we take a relativistic version [10], which can be written as

$$G(p^0,\boldsymbol{p}) = \frac{M}{E(\boldsymbol{p})}\sum_r u_r(\boldsymbol{p})\bar{u}_r(\boldsymbol{p})\left[\int_{-\infty}^{\mu} d\,\omega \frac{S_h(\omega,\boldsymbol{p})}{p^0-\omega-i\eta} + \int_{\mu}^{\infty} d\,\omega \frac{S_p(\omega,\boldsymbol{p})}{p^0-\omega+i\eta}\right], \tag{25}$$

$S_h(\omega,\boldsymbol{p})$ and $S_p(\omega,\boldsymbol{p})$ being the hole and particle spectral functions respectively, which are taken from the work of [10,29].

We use the local density approximation in which the spectral functions depend on the density of the point of the nucleus at which they are evaluated. In our formalism we use spectral functions for symmetric nuclear matter. The normalization of the hole spectral function is given by

$$4\int d^3r \int \frac{d^3p}{(2\pi)^3}\int_{-\infty}^{\mu} S_h(\omega,\boldsymbol{p},k_F(\boldsymbol{r}))\,d\omega = A\,, \tag{26}$$

where $k_F(\boldsymbol{r}) = [3\pi^2\rho(\boldsymbol{r})/2]^{1/3}$ is the local Fermi momentum at the point $\boldsymbol{r}$. All our calculations are done for ^{56}Fe. The density for this nucleus is expressed as a two Fermi parameter distribution given in [30].

We now calculate $\mathrm{Im}\,\Pi^{\alpha\beta}(q)$ by using Cutkosky rules, Eq. (21), the expression of Eq. (25) for the nucleon propagator in the medium, free propagators for particles in the final state and by means of Eq. (23) we have the hadronic tensor

$$W_A^{\alpha\beta} = 4\int d^3r \int \frac{d^3p}{(2\pi)^3}\frac{M}{E(\boldsymbol{p})}\int_{-\infty}^{\mu} dp^0 S_h(p^0,\boldsymbol{p})W_N^{\alpha\beta}(p,q)\,. \tag{27}$$

In order to evaluate F_{3A}, we calculate the components xy on both sides of Eq. (27). We have, using $\epsilon_{0123}=1$, and taking $\boldsymbol{q}$ along the z axis, as usual,

$$W_A^{xy} = -\frac{i}{2M_A}q_z W_{3A}\,, \tag{28}$$

and for the right hand side we will have for the moving nucleon

$$W_N^{xy} = \frac{p_x p_y}{M^2}W_{2N}(p,q) + \frac{i}{2M^2}W_{3N}[p_z q_0 - p_0 q_z]\,. \tag{29}$$

Since we have

$$q_0 W_{3A} = F_{3A}(x)\,,$$
$$\frac{pq}{M}W_{3N}(p,q) = F_{3N}(x_N)\,, \tag{30}$$

with x as defined in Eq. (9) and x_N is the Bjorken variable expressed in terms of the nucleon variables , $(p^0,\boldsymbol{p})$, in the nucleus

$$x_N = \frac{Q^2}{2pq}\,, \tag{31}$$

we obtain the expression for $F_{3A}(x)$ in the Bjorken limit

$$\frac{F_{3A}(x)}{A} = 4\int d^3r \int \frac{d^3p}{(2\pi)^3} \frac{M}{E(\boldsymbol{p})} \int_{-\infty}^{\mu} dp^0 S_h(p^0,\boldsymbol{p}) \frac{x_N}{x} \left[\frac{p_0 q_z - p_z q_0}{M q_z}\right] F_{3N}(x_N)\,, \tag{32}$$

where the contribution of W_2 appearing in Eq. (29) vanishes after momentum integration.

Defining γ as

$$\gamma = \frac{q_z}{q^0} = \left(1 + \frac{4M^2x^2}{Q^2}\right)^{1/2}\,, \tag{33}$$

we get

$$\frac{F_{3A}(x)}{A} = 4\int d^3r \int \frac{d^3p}{(2\pi)^3} \frac{M}{E(\boldsymbol{p})} \int_{-\infty}^{\mu} dp^0 S_h(p^0,\boldsymbol{p}) \left(\frac{p_0\gamma - p_z}{(p_0 - p_z)\gamma}\right) F_{3N}(x_N) \tag{34}$$

IV. RESULTS AND CONCLUSION

We begin by showing the results for $R_3 = F_{3A}/AF_{3N}$ and comparing them with the corresponding ratio $R_2 = F^l_{2A}/AF^l_{2N}$ in Fig. 3. For F_{3N} and F^l_{2N} we have taken the parametrization of [31]. For the meson structure functions that contribute to R_2 we have used the parametrization given in [32]. We can see some similarities in the region around $x = 0.5 \sim 0.6$ where the ratio is smaller than unity and which is mostly due to nuclear binding effects, as discussed in detail in [8,10]. Similarities in the region of $x > 0.6$, where the ratio shows a fast increase, are also apparent, and they are mostly due to the effect of Fermi motion [7,10]. The differences between the neutrino and charged lepton ratios are more important at values of $x < 0.6$. These differences are mostly due to the lack of meson renormalization effects in the neutrino structure function, as can be seen in the figure, where we also show the results for R_2 without the meson renormalization effects.

We should note that the nuclear effects are sizeable, with values of R_3 around 0.8 in the region of $x \simeq 0.6$ and around 0.9 for low values of x. These nuclear corrections are considerably larger than those found for the deuteron [16], as it was also the case for R_2 in the charged lepton case.

In Fig. 4 we show results for R_3 for different values of Q^2. We observe that for low values of x the results for R_3 are rather independent of Q^2, but this is not the case at large values of x, where there are substantial differences. Given the fact that the most important contribution to the GLS sum rule comes from the values of $x < 0.4$, the results of the figure indicate that nuclear effects can reduce the GLS sum by about 10%. Since one of the purposes of this work is to facilitate the task of experimentalists in analyses of the GLS sum rule and other QCD predictions for F_{3N}, we provide here an easy parametrization of R_3 which can serve to induce the results for F_{3N} from the measured nuclear data of F_{3A}. In table I we give the parameters of a fit of the ratio $R_3(x)$ for the Q^2 values of 5, 30 and 50 GeV^2. The form used is $R_3(x) = A(B-x)^\alpha/(1-x)^\beta$. For larger values of Q^2 results are similar to those for 50 GeV^2.

We also want to stress that the factor $(p_0\gamma - p_z)/(p_0 - p_z)\gamma$ appearing in Eq. (34) which goes to unity in the Bjorken limit (see Eq. (33)), is not negligible for values of $Q^2 \approx 4M^2$ and produces changes of around 10% in R_3 for values of $x \approx 0.8 - 1$ at $Q^2 = 5$ GeV^2.

In Fig. 5 we compare our results with those of Kulagin [17] and ST [16]. It is quite clear that both for the case of Kulagin and the present results the differences with the deuteron results of ST are significant. Our results and those of Kulagin are qualitatively similar around $x \approx 0.4 - 0.5$, but they divert from each other both at large x and small x. The discrepancies at large x are not surprising since it was shown in [33] that the results for F_{2A} at large x were very sensitive to the parametrization used for F_{2N}, which is different in [17] and the present case. These differences, however, should not be very relevant for tests of the GLS sum rule, since the contribution to the sum rule from the region of $x > 0.6$ is very small. The discrepancies for values of $x < 0.4$ are more relevant in connection with this sum rule since 10% effects, typical differences at low x between both approaches, are of the same order of magnitude as the QCD corrections to the GLS. The main reason for the discrepancies in the two results should be seen from the different approaches followed. In [17] the spinors are normalized in a way to force baryon number conservation in a non relativistic formalism, in line of the idea of the flux factor of [21] to introduce relativistic corrections in a nonrelativistic formalism. The advantage of the present work is that it uses a relativistic formalism from the beginning, in which baryon number conservation is automatically fulfilled. The differences of 10% in the region of small x between the two aproaches is about the same one as found between our approach and those using the flux factor in studies of F^l_{2A} [10,18].

In summary, we present here results for R_3 based on a relativistic approach and the use of an accurate nuclear spectral function which reproduces nuclear bindings, momentum distributions, etc. Within this formalism we were able to reproduce the EMC effect for different nuclei and the experimental results of F_{2A} in the region of $x > 1$. We have used here the same formalism to evaluate F_{3A}. There are some differences with respect to F_{2A} in the nuclear effects, mostly due to the absence of meson renormalization corrections in F_{3A}. The results obtained are parametrized in an easy way to facilitate future analyses of experimentalists in order to deduce the elementary F_{3N} structure function from the nuclear measurements and be able to test QCD corrections and obtain reliable values of α_s.

ACKNOWLEDGMENTS

We would like to acknowledge W. Seligman for providing us with a copy of his Ph. D. Thesis and interesting comments. One of us, S.K.S. wishes to acknowledge financial support from Ministerio de Educación y Cultura in his sabbatical stay in Valencia. E.M. wishes to acknowledge financial support from the Ministerio de Educación y Cultura. This work is partially supported by DGICYT, contract no. PB96-0753.

REFERENCES

* Permanent Address: Physics Department, Aligarh Muslim University, Aligarh, India 202002.

[1] M. Conrad, M.H. Shaevitz and T. Bolton, hep-ex/9707015.
[2] W.G. Seligman et al., Phys. Rev. Lett. **79**, 1213 (1997).
[3] J.J. Aubert et al., Phys. Lett. **B123**,275 (1983).
[4] R.P. Bickerstaff and A.W. Thomas, J. Phys. G **15**, 1523 (1989).
[5] M. Arneodo, Phys. Rept. **240**, 301 (1994).
[6] D.F. Geesaman, K. Saito and A.W. Thomas, Annu. Rev. Nucl. Part. Sci. **45**, 337 (1995).
[7] A. Bodek and J.L. Ritchie, Phys. Rev. D **23**, 1070 (1981).
[8] S.V. Akulinichev, S.A. Kulagin and G.M. Vagradov, Pis' ma Zh. Eksp. Teor. Fiz **42**, 105 (1985); JETP Lett. **42**, 127 (1985); Phys. Lett. **158B**, 485 (1985).
[9] M. Ericson and A. W. Thomas, Phys. Lett. **128B**, 112 (1983).
[10] E. Marco, E. Oset and P. Fernández de Córdoba, Nucl. Phys. **A611**, 484 (1996).
[11] G.T. Jones et al., Z. Phys. C **62**, 575 (1994).
[12] M. Diemoz, F. Ferroni, E. Longo and G. Martinelli, Z. Phys. C **39**, 21 (1988).
[13] A.D. Martin, W.J. Stirling and R.G. Roberts, Phys. Rev. D **47**, 867 (1993).
[14] H.L. Lai, J. Botts, J. Huston, J.G. Morfin, J.F. Owens, J.W. Qiu, W.K. Tung and H. Weerts, Phy. Rev. D **51**, 4763 (1995).
[15] R.G. Roberts, *The structure of the proton* (Cambridge University Press, Cambridge, 1990), p. 41.
[16] A.V. Sidorov and M.V Tokarev, Phys. Lett. **B358**, 353 (1995).
[17] S.A. Kulagin, nucl-th/9801039.
[18] C. Ciofi degli Atti and S. Liuti, Phys. Rev. C **41**, 1100 (1990).
[19] V.V. Burov and A.V. Molochkov, nucl-th/9703008.
[20] D.J. Gross and C.H. Llewellyn Smith, Nucl. Phys. **B14**, 337 (1969).
[21] L.L. Frankfurt and M.I. Strikman, Phys. Lett. **B183**, 254 (1987).
[22] W.G. Seligman Ph.D. thesis, Nevis Report 292, 1997.
[23] D.A. Harris, hep-ex/9506010.
[24] P. Fernández de Córdoba, E. Marco, H. Müther, E. Oset and A. Faessler, Nucl. Phys. **A611**, 514 (1996).
[25] S.M. Bilenky, *Introduction to Feynman diagrams in electroweak interactions physics* (Editions Frontiers, Gif-sur-Yvette, 1994).
[26] G. Altarelli and G. Parisi, Nucl. Phys. **B126**,298 (1977); V.N. Gribov and L.N. Lipatov, Sov. J. Nucl. Phys. **15**,438 (1972); Yu. L. Dokshitzer, Sov. Phys. JETP **46**, 641 (1977).
[27] S.A. Larin and J.A.M. Vermaseren, Phys. Lett. **B259**, 345 (1991).
[28] C. Itzykson and J.B. Zuber, *Quantum field theory* (McGraw-Hill, New York, 1980).
[29] P. Fernández de Córdoba and E. Oset, Phys. Rev. C **46**, 1697 (1992).
[30] H. de Vries, C.W. de Jager and C. de Vries, At. Data Nucl. Data Tables **36**, 583 (1971).
[31] A.D. Martin, W.J. Stirling and R.G. Roberts, Phys. Rev. D **51**, 4756 (1995).
[32] M. Glück, E. Reya and A. Vogt, Z. Phys. C **53**, 651 (1992).
[33] E. Marco and E. Oset, Nucl. Phys. **A618**, 427 (1997).

TABLES

TABLE I. Fits of the ratio $R_3(x, Q^2) = F_{3A}(x, Q^2)/AF_{3N}(x, Q^2)$ for different values of Q^2. The form of the fit is $R_3(x) = A(B - x)^{\alpha}/(1 - x)^{\beta}$

Q^2 (GeV^2)	A	B	α	β
5	0.691	1.29	1.21	0.688
30	0.647	1.06	6.88	6.19
50	0.599	1.07	6.43	5.64

FIGURES

FIG. 1. Diagram for the process of deep inelastic neutrino-nucleon scattering.

FIG. 2. Self-energy diagram of the neutrino in the nuclear medium associated with the process of deep inelastic neutrino-nucleon scattering.

FIG. 3. Solid line: results for the ratio $F_{3A}(x)/AF_{3N}(x)$; dashed line: results for the ratio $F^l_{2A}(x)/AF^l_{2N}(x)$ including the contribution of the nucleons and the mesons; dotted-dashed line: results for the ratio $F^l_{2A}(x)/AF^l_{2N}(x)$ including only the contribution of the nucleons. All curves are evaluated at $Q^2 = 50$ GeV^2.

FIG. 4. Results for the ratio $F_{3A}(x)/AF_{3N}(x)$ at different values of Q^2. Dotted-dashed line: ratio at $Q^2 = 50$ GeV^2; long dashed line: ratio at $Q^2 = 30$ GeV^2; solid line: ratio at $Q^2 = 5$ GeV^2; short dashed line: ratio at $Q^2 = 5$ GeV^2 but setting γ equal to 1 in Eq.(34).

FIG. 5. Results for the ratio $F_{3A}(x)/AF_{3N}(x)$ at $Q^2 = 5$ GeV^2 by different authors. Solid line: this work; dashed line: Kulagin [17]; dotted-dashed line: Sidorov and Tokarev [16] (for deuteron).

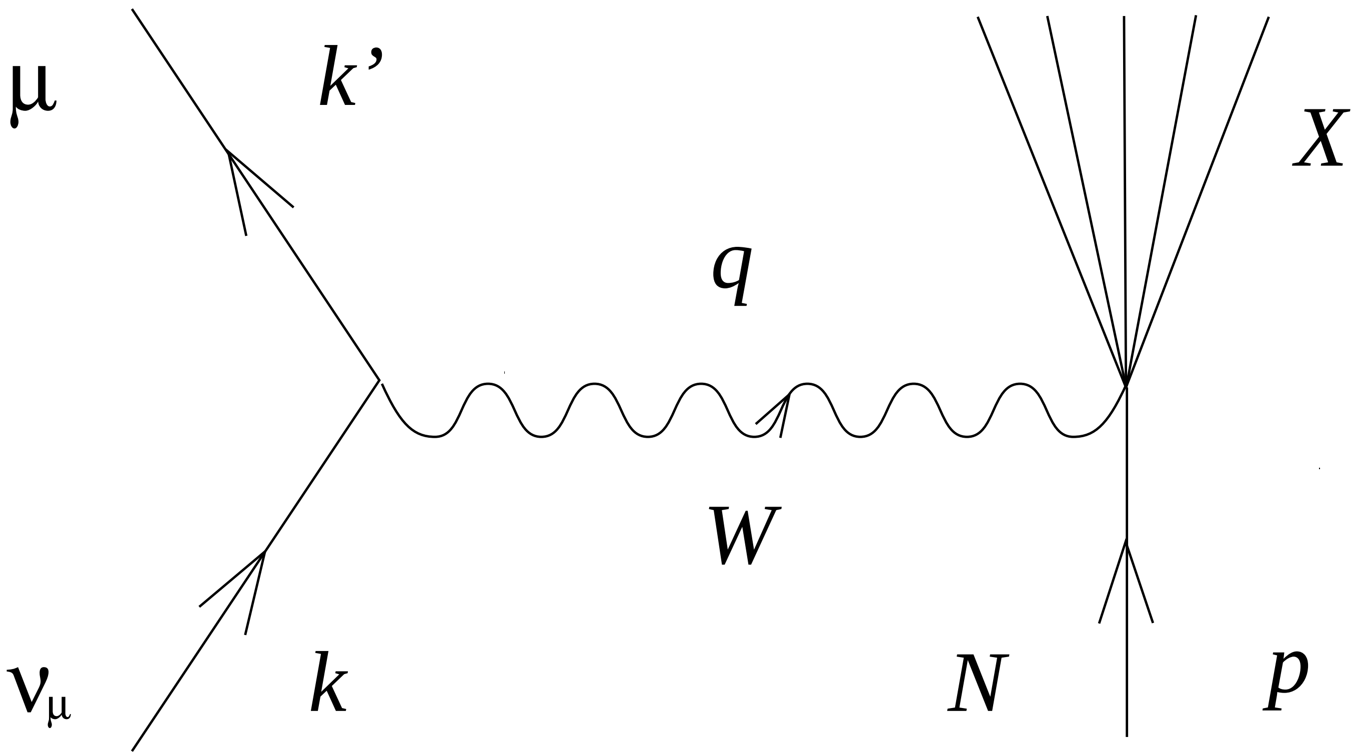

μ
k'
X
q
W
ν_μ
k
N
p

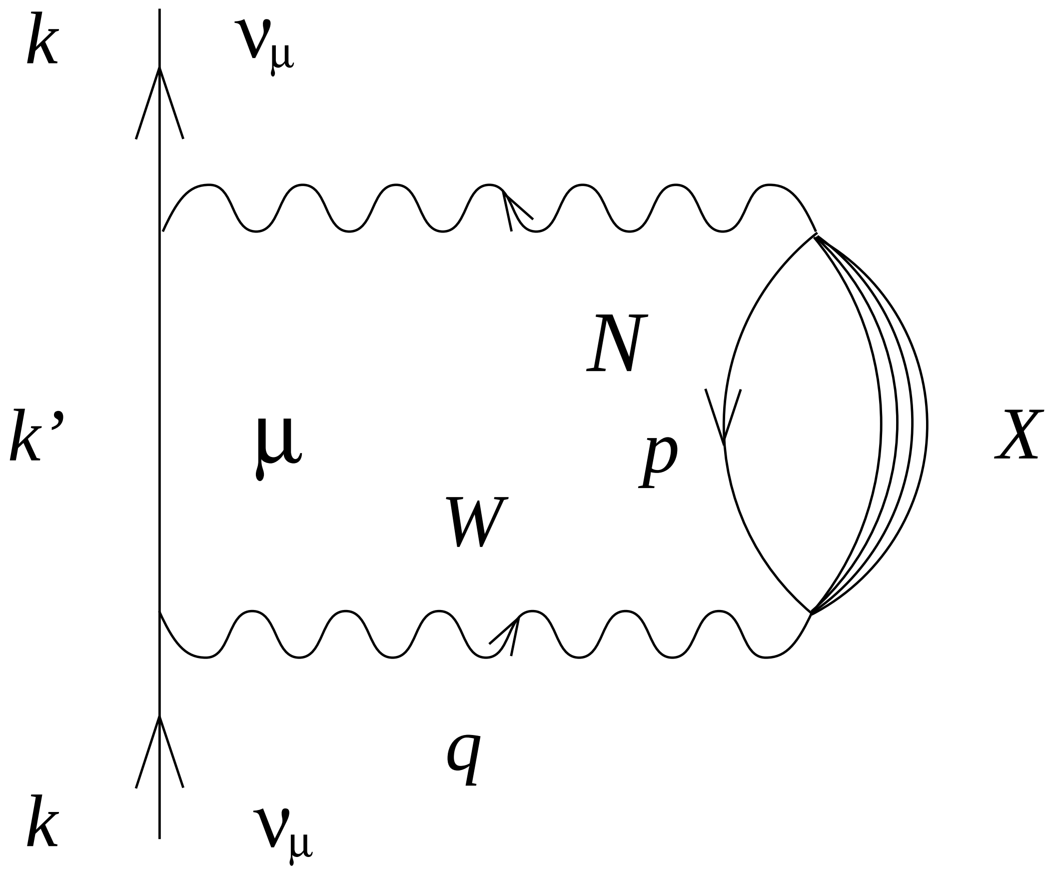

k
ν_μ
N
k'
μ
p
X
W
q
k
ν_μ

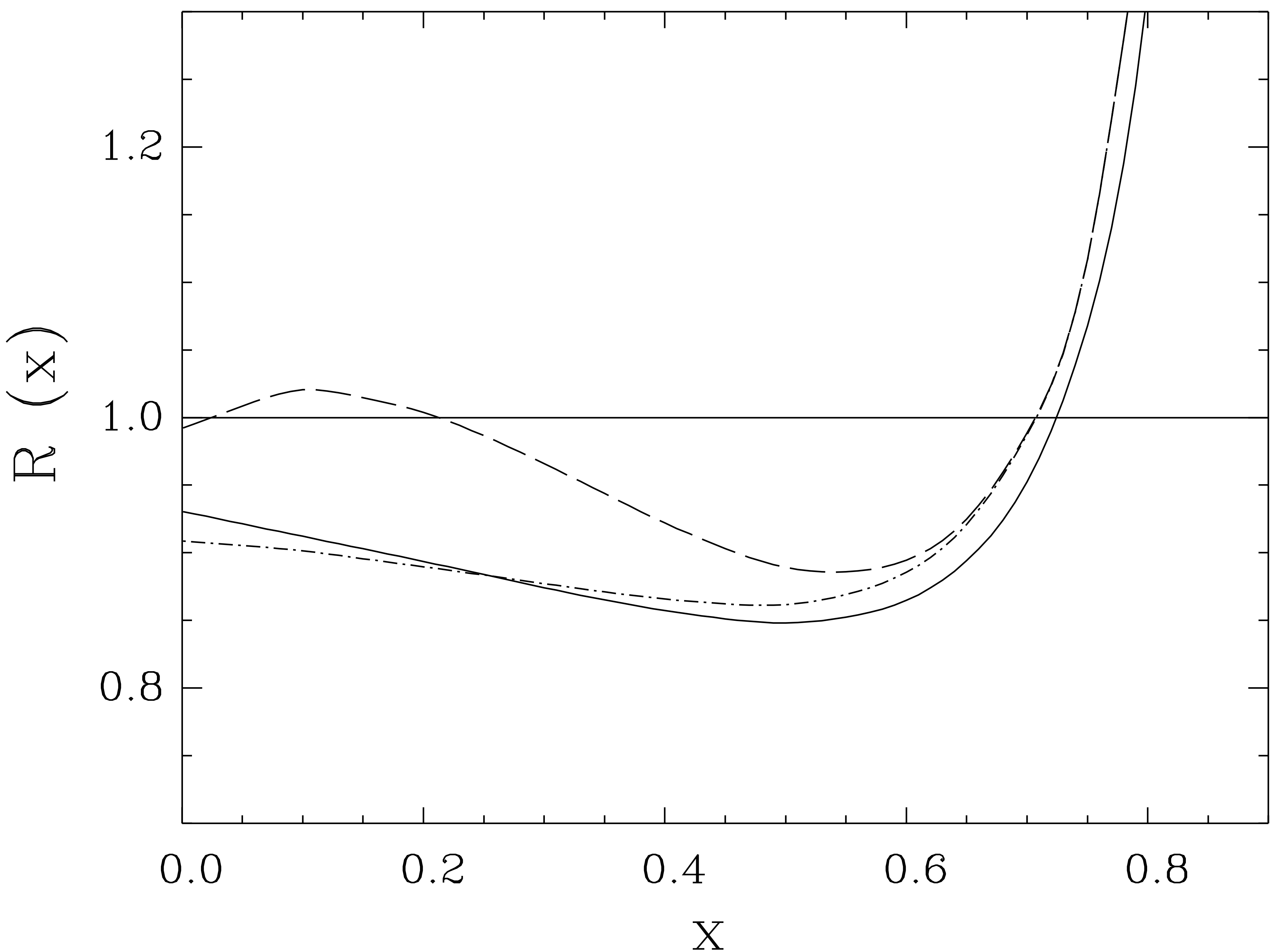
R (x)
1.2
1.0
0.8
0.0
0.2
0.4
0.6
0.8
X

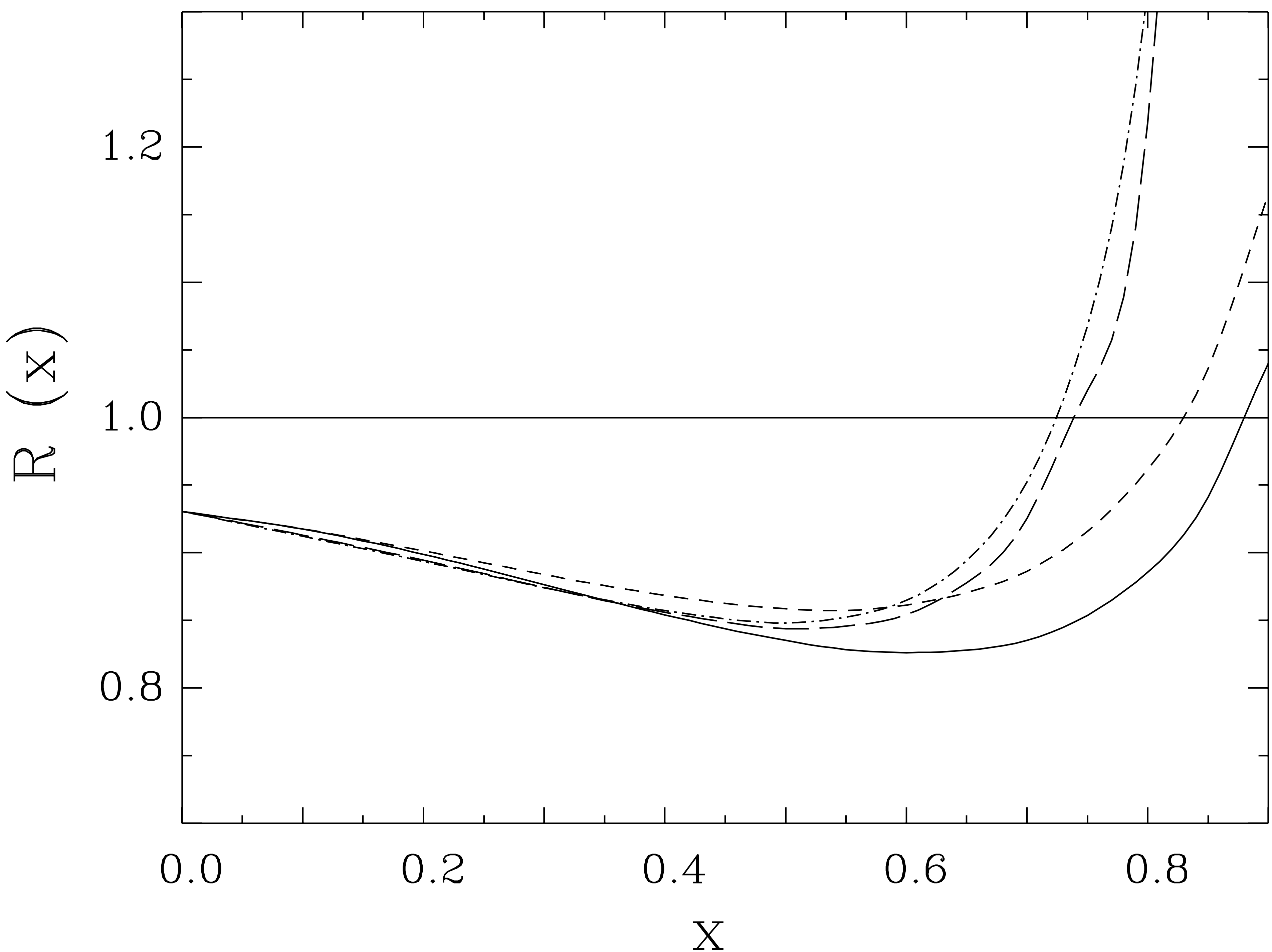

R (x)
1.2
1.0
0.8
0.0
0.2
0.4
0.6
0.8
X

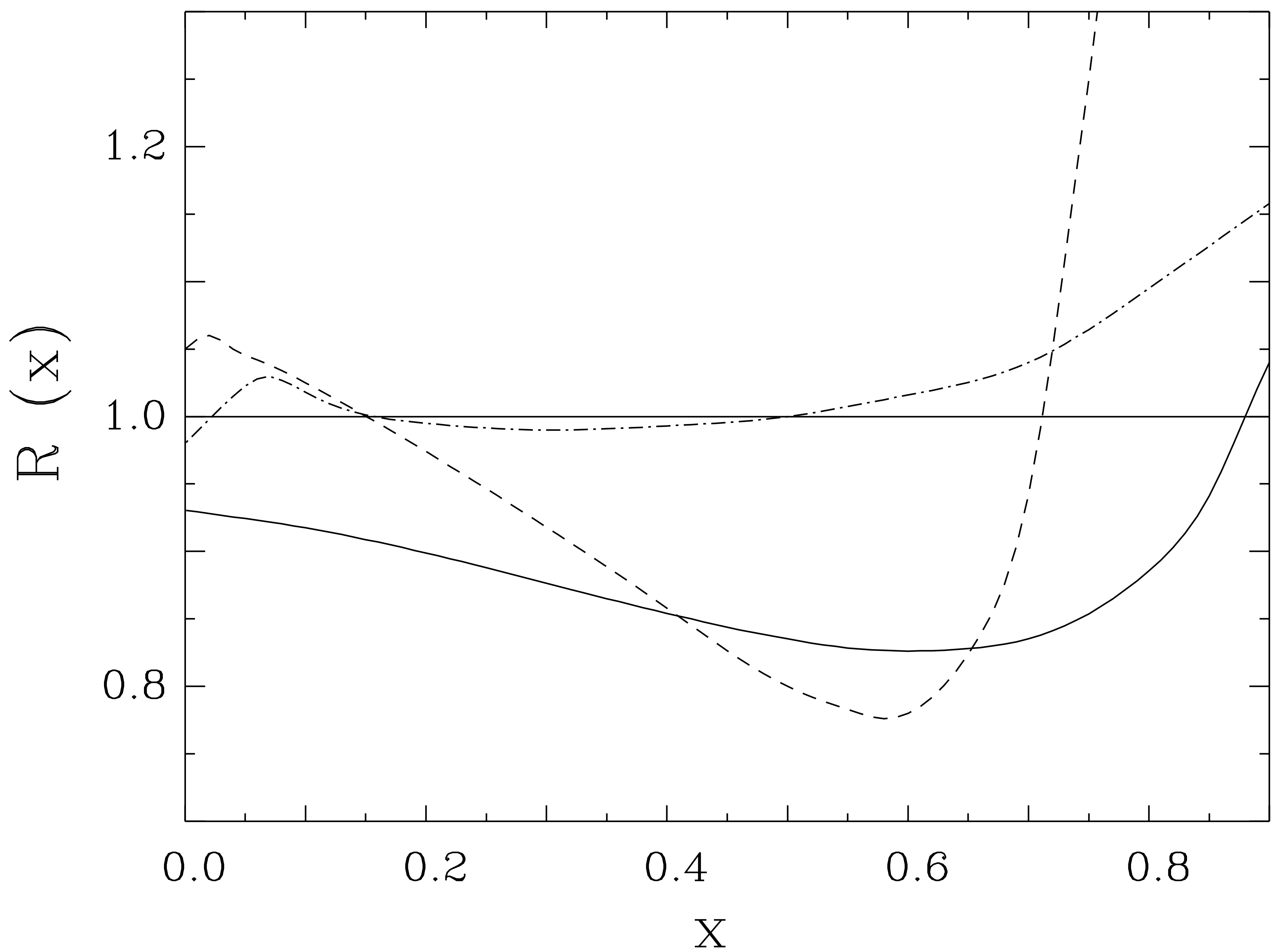

R (x)
1.2
1.0
0.8
0.0
0.2
0.4
0.6
0.8
X